

# Self-assembly of anisotropic soft particles in two dimensions

Daniel Salgado-Blanco and Carlos I. Mendoza\*

Instituto de Investigaciones en Materiales, Universidad Nacional Autónoma de México, Apdo. Postal 70-360, 04510 México, D.F., Mexico

October 21, 2018

## Abstract

The self assembly of core-corona discs interacting via anisotropic potentials is investigated using Monte Carlo computer simulations. A minimal interaction potential that incorporates anisotropy in a simple way is introduced. It consists in a core-corona architecture in which the center of the core is shifted with respect to the center of the corona. Anisotropy can thus be tuned by progressively shifting the position of the core. Despite its simplicity, the system self organize in a rich variety of structures including stripes, triangular and rectangular lattices, and unusual plastic crystals. Our results indicate that the amount of anisotropy does not alter the lattice spacing and only influences the type of clustering (stripes, micells, etc.) of the individual particles.

## 1 Introduction

Simple pair potentials are often used to describe effective interactions among substances with supramolecular architecture [1, 2]. Frequently, this is done considering models of particles consisting of a hard core surrounded by a repulsive soft corona. In such representations, the interactions between the so called core-shell or core-corona particles, are treated in an effective way that takes into consideration the entropy of the brush-like coronas surrounding each core. The simplest of them consists of a hard core surrounded by a square shoulder [3, 4]. Its simplicity allows to predict, based on geometrical arguments, under which circumstances a given family of structures is obtained. Among the physical systems described using this model we can mention colloidal particles with block-copolymers grafted to their surface where self-consistent field calculations lead to effective interactions that can be modeled by a square-shoulder potential [5]. Such interactions can be controlled by adjusting the length, species, the

---

\*E-mail: cmendoza@iim.unam.mx

grafting density of the grafted polymers, the quality of the solvent, the density and location of the hydrogen bonding, etc.

The phase behavior and associated pattern formation of two-dimensional systems with core-shell architecture has been studied by using numerical simulations. These studies have shown that single component softened-core repulsive potentials may give rise to stripe phases [3]-[8] and periodic structures that are explained in terms of the competing interactions between the hard core and the soft shoulder. Binary mixtures of cylindrically symmetric core-shell particles in two dimensions in which particles of the same species interact through a repulsive shoulder while particles of different species interact via an attractive square well have also been studied [9]. It is found that the larger number of control parameters inherent to the mixture allows to extend the ensemble of possible self-assembled structures, originating structures like stripes, square lattices as well as other more sophisticated arrangements [9]. In spite of the rich variety of self-organized structures found in the single and two-species systems of particles with isotropic shapes and interactions, there are intrinsic limitations associated with their isotropy [10]. In order to circumvent such limitations, active research has been done in order to incorporate anisotropy in the building blocks. Additionally, the unprecedented revolution in particle syntheses, which has led to the possibility to modify chemically the surface of the particles as well as to build an amazing variety of building blocks of different shapes, compositions, patterns and functionalities, offers a multitude of molecular designs for particles with unique properties that are amenable to self-assembly [11, 12]. A broad range of investigations has been focused on the fabrication of non-spherical colloidal particles as well as their application for drug delivery, molecular imaging and self-assembly (see [10] and references therein). A variety of interesting and efficient techniques to synthesize particles with different shapes have been devised in recent years. Among them we can mention stretching methods, micromolding, microfluidic approaches and methods using seeded polymerization [10]. As a consequence, it is now recognized that particles with anisotropic shape or interacting via anisotropic potentials are powerful tools for engineering the assembly of particular targeted structure and therefore have been actively investigated in recent years [12, 13]. These types of colloidal particles have attracted increasing attention because of their promising properties for applications in nanotechnology, electronics, biotechnology and others. In particular, much work have been done on rod-shaped particles [14, 15] two-faced (Janus) [16]-[18] and patchy particles [19]-[27].

Recently, Vanakaras has proposed a special class of two-dimensional Janus core-corona system that spontaneously form exotic and thermodynamically stable structures not seen in systems of isotropic particles [11]. This and other studies, together with the large variety of experimental techniques to fabricate core-shell and anisotropic particles suggest that 2D anisotropic core-shell particles are promising candidates for bottom-up design of precise two-dimensional templates.

Regardless of the myriad of possible shapes and interactions that different anisotropy building blocks may have, all of them can be conveniently classified

in three different types [13], (1) shape anisotropy + interaction isotropy; hard-rods belong to this class, (2) shape anisotropy + interaction anisotropy, for example, Gay-Berne [28] and patchy ellipsoids, and finally (3) shape isotropy + interaction anisotropy, as in the case of spheres interacting through a dipolar electric field. In what follows, we are going to introduce a model for anisotropic particle of the type 3.

The aim of this paper is to propose a minimal model that incorporates in a simple way the effects of anisotropy on the self assembly of colloidal particles that interact via core-shell potentials. We study by computer simulation the self-assembled structures obtained at zero temperature for a collection of two-dimensional particles consisting of a non concentric core-corona architecture. Despite its simplicity, the rich pattern formation arising from the self organization indicates the importance of the interaction anisotropy on these core-corona systems. Among the rich variety of patterns encountered, we can highlight the formation of stripes, rectangular arrays, triangular lattices, and unusual plastic crystal phases. It is also found that anisotropy may promote the stripe formation in some cases or inhibit their formation in others, however, the degree of anisotropy does not alter the lattice spacing. These results suggest a strategy for producing a range of self-assembled structures which could be exploited for use as templating or directing agents in materials syntheses.

## 2 System and Methods

The system consists of particles interacting through an anisotropic pair potential  $V(r)$  composed of an impenetrable core of diameter  $\sigma_0$  surrounded by an adjacent square shoulder with range  $\lambda\sigma_0$  similar to existing representations used to describe isotropic branched particles [2]. In order to incorporate interaction anisotropy in this model, we propose to shift the center of the core with respect to the center of the corona as sketched in Fig. 1. Mathematically, this potential can be expressed as

$$V(r) = \begin{cases} \infty, & \text{if core-core distance} \leq \sigma_0 \\ \varepsilon, & \text{if corona-corona distance} \leq \lambda\sigma_0 \\ 0, & \text{otherwise} \end{cases}, \quad (1)$$

where  $r$  represents the core-core distance for the infinite repulsive part of the potential, and the corona-corona distance for the repulsive square shoulder of energy  $\varepsilon$ . The only restriction for the distance  $d$  between the centers of the core and the corona of a given particle is that the core remains completely contained inside the corona, that is,  $d \leq d_{max}$ , where  $d_{max} = \sigma_0(\lambda - 1)/2$ . In order to maintain the interparticle potential as simple as possible, we have assumed that there is no core-corona interaction. This model could represent in an approximate way a branched particle in which the length of the branches is larger in one direction than in the opposite one. The parameter  $\delta \equiv d/d_{max}$  is introduced to quantify the displacement of the core with respect to the corona. Because  $0 \leq d \leq d_{max}$ , then the reduced shift  $\delta$  assumes values in the interval

$0 \leq \delta \leq 1$ . When  $\delta = 0$ , the shift is zero and the particle is a regular isotropic core-corona disk. At the other extreme, when  $\delta = 1$ , the shift is maximum and the central disk representing the core is tangent from inside to the disk representing the corona. Because of the different positions of the core and corona, the cylindrical symmetry of the disk is broken, imparting anisotropy to the particles.

Standard Monte Carlo simulations based on the canonical ensemble (NVT simulations) in a square box of side  $L$  with periodic boundary conditions have been carried out using the Metropolis algorithm. We have used  $\sigma_0$  and  $\varepsilon$  as length and energy units, respectively, the reduced temperature  $T^* = k_B T / \varepsilon$ , where  $k_B$  is Boltzmann's constant; the reduced number density  $\rho^* = N \sigma_0^2 / L^2$  and the reduced displacement of the center of the core from the center of the corona  $\delta$ , as defined above. We have studied the pattern formation dependence on  $\delta$ , for different choices of  $\lambda$  and  $\rho^*$ . Simulations are performed with  $N = 1000$  particles and control runs with  $N = 5000$  particles to exclude finite size effects were also done. In all cases, the system is first disordered at high temperature and then brought from  $T^* = 0.4$  to the final temperature  $T^* = 0.01$  through an accurate annealing procedure with steps of 0.01. An equilibration cycle consisted, for each temperature, of at least  $2 \times 10^8$  MC steps, each one representing one trial displacement and rotation of each particle, on average. At every simulation step a particle is picked at random and given a uniform random trial displacement within a radius of  $0.5\sigma_0$  and a random trial rotation within an angle of  $\pm 0.1\pi$ . If we are simulating inside a two-phase coexistence region of the phase diagram, we can not exclude the possibility that the simulation do not show the phase separation. This is due to the fact that in NVT simulations the system may be kept at a density where it would prefer to separate into two phases of different densities but is prevented from doing so by finite-size effects. For this reason, we have completed our investigation by studying the behavior of our model system through simulations at constant number of particles, pressure  $P$ , and temperature (NPT simulations). In this case, the system is free to transform completely into the state of lower free energy [29].

A variety of interesting structural features of this simple model at low temperatures are in evidence in Fig. 2, where a few of them are exhibited for  $\lambda = 2.5$  and  $\rho^* = 0.291$ . This set of parameters is chosen as to agree with the ones used by Malescio and Pellicane in Ref. [2] to obtain lane formation. Panel (a) shows a stripe pattern obtained for isotropic particles,  $\delta = 0$ . We observe that both, the interparticle distance in a given lane and the lane to lane spacing is determined by the corona diameter. The particle-particle distance in a given lane is such that the coronas of each other particle just touch for the given set of parameters. Analogously, the lane to lane distance is such that the coronas of adjacent lanes barely touch. The system adopts this array in order to minimize unfavorable overlaps between coronas. As we progressively increase the anisotropy parameter,  $\delta$ , the system adopts alternative structural motifs. For a small value of the reduced displacement,  $\delta = 0.2$ , the system organize in a pattern formed by two distinct phases. The first one corresponds to the same lane pattern observed in panel (a) but this phase co-exists with an

approximately triangular array of compact clusters or aggregates made mainly of dimers and trimers. Particles that belong to a given cluster are located such that their coronas overlap as much as possible. The limiting factor that prevents the total collapse of such aggregates are their hard-cores thus conferring a non-cylindrically symmetric shape to the envelope of the coronas of the resulting aggregates. For example, the aggregates of trimers in Fig. 2b have triangular shapes as well as the envelope of their coronas. On the other hand, the lattice parameter for the lattice of clusters is such that the coronas of different clusters do not overlap. This fact not only determine the lattice parameter but, in complicity with the non cylindrically symmetric shape of the cluster's coronas, also induces a orientational correlation between different aggregates. Increasing even more the value of the reduced displacement to  $\delta = 0.3$ , the phase corresponding to the stripes has disappeared completely and only an approximately crystalline arrangement consisting of a triangular lattice of dimers and trimers remains. Finally, at the maximum displacement,  $\delta = 1$ , the regular lattice of correlated dimers and trimers is replaced by an ordered array of clusters, each one formed by two or three particles whose coronas completely overlap but with the position of their cores completely uncorrelated with the ones of the other aggregates. In other words, the coronas that belong to an aggregate of particles overlap almost perfectly forming an isotropic corona for the resultant aggregate. This allows each aggregate to rotate freely and independently of the other aggregates thus forming an unconventional plastic crystal with long range (or quasi-long range) translational but no orientational correlations. We say it is an unconventional plastic crystal since usually the term refers to an array with translational order but without correlations between the orientation of the molecules. Here, the lack of orientational correlations is translated into a lack of positional correlations between the cores. It is interesting to note that the incorporation of anisotropy has inhibited the stripe formation for this set of parameters.

Figure 3 shows a sequence of spatial configurations (top panels) for  $\lambda = 3$  and  $\rho^* = 0.5$ . As the relative displacement is increased, the system turns from the staggered pattern of panel (a), where the (isotropic) particles are arranged in quasiclump states with the center of the particles occupying the lattice points of a subtriangular lattice (see inset), to a lane conformation, for  $\delta = 0.166$ , where each lane is constituted by two adjacent rows of particles whose arrangement resemble a succession of parallel dumbbells (Fig. 3b, top). The fact that the particle's cores within a given stripe do not locate in a triangular sublattice indicate that clustering is not close-packed in this case, in sharp contrast with the case of isotropic potentials where clusters of close-packed particles are predicted [30]. The spacing between consecutive lanes is dictated by the condition that the coronas of adjacent lanes do not overlap, as shown in the respective inset. With a further increase of anisotropy ( $\delta = 0.333$ ), the system turns into a triangular lattice of hexagonal clumps formed by seven particles whose cores are located on a triangular sublattice, as shown in the inset of Fig. 3c (top). Finally, for the maximum anisotropy ( $\delta = 1$ ), the almost perfect crystal lattice transforms into an unconventional plastic crystal made of a regular lattice of discotic aggregates

of mostly five particles which are orientationally uncorrelated with the particles forming other aggregates. Actually, in this case, the presence of the cores do not influence the structure of the coronas, the same triangular lattice of coronas would be obtained even if no cores were present. Contrary to the case analyzed in Fig. 2, for this set of parameters, the stripe formation is first promoted by the addition of anisotropy (transition from Fig. 3a to Fig. 3b) and then suppressed (transition from Fig. 3b to Fig. 3c). As seen, incorporation of anisotropy has a profound effect in the final structure obtained.

We analyze the structural order of our system by looking at the diffraction patterns (Fig. 3, central panels) and through the orientationally averaged radial correlation function,  $g(r)$ , which gives the probability to find a pair of molecules at a distance between  $r$  and  $r + dr$  (Fig. 3, bottom panels). In the case of isotropic particles (Fig. 3a),  $g(r)$ , is the same for the core and corona centers, as depicted by the blue and red lines, respectively, of Fig. 3a bottom panel. Clearly a long-range order is present with two large peaks, the first one located near the core diameter  $r \approx \sigma_0$ , showing that the first coordination shell is formed by particles whose cores are nearly touching, compatible with the snapshot of Fig. 3a. The second large peak is located near the soft-shoulder diameter  $r \approx \lambda\sigma_0$ , showing that the outer lattice spacing is determined by the corona diameter. Intermediate peaks located near  $r \approx 2\sigma_0$ , indicates that the second coordination shell consists of particles located at twice the core diameter, consistent with the fact that the underlying triangular lattice is not completely filled, otherwise, peaks located near  $r \approx \sqrt{3}\sigma_0$ , would be present. In Fig. 3b bottom panel we show  $g(r)$ , for a small anisotropy,  $\delta = 0.166$ . Since the center of the cores do not coincide with the center of the coronas, then there will be a  $g(r)$  for the cores and a different one for the coronas. Although  $g(r)$  for the cores still present moderate long-range correlations (blue line), its peak structure is less pronounced with the exception of the first peak, as a result of a slightly more disordered arrangement. In contrast, the peak structure of  $g(r)$  for the coronas (red line) is very pronounced indicating the presence of long-range order. Notice that the first peak appears below  $r = \sigma_0$  due to the fact that the relative displacement  $\delta > 0$  allows the center of the coronas to approach closer. The large peak around  $r \approx \lambda\sigma_0$  is the signature of the interlane spacing which is, again, imposed by the shoulder width. At the next case considered,  $\delta = 0.333$ , the shape of  $g(r)$  still presents considerable structure as shown in Fig. 3c, bottom panel (blue line). The first coordination shell is well pronounced and the second and third peaks, near  $r \approx \sqrt{3}\sigma_0$  and  $r \approx 2\sigma_0$ , correspond to the second and third nearest neighbors. The broader peaks in  $g(r)$  represent correlations between particles belonging to different aggregates. The larger anisotropy of this case ( $\delta = 0.333$ ), allows a larger interpenetration of the coronas belonging to the same aggregate, a fact which is reflected by the first broad structured peak in  $g(r)$  for the coronas, as shown in Fig. 3c bottom panel (red line). The second broad peak appearing near  $r \approx \lambda\sigma_0$ , corresponds to the first coordination shell of the triangular lattice formed by the aggregates. Finally, in Fig. 3d, bottom panel we show  $g(r)$  for the largest anisotropy ( $\delta = 1$ ). An oscillatory form, typical of a liquid-like structure, is seen in the case of the cores (blue line)

with only a few correlation layers. On the other hand, the triangular lattice of overlapped coronas with lattice constant  $\lambda\sigma_0$  is clearly reflected by the peaks at  $r \approx 0$  and  $r \approx \lambda\sigma_0$  (red line). Therefore, in this last case, the liquid-like structure of the cores coexist with a triangular lattice of overlapped coronas. This characteristic suggest the possibility of using this self-assembled structure as a template to tailor materials with hybrid properties at the nanoscale, those of an amorphous material (associated with the cores) mixed with those of a crystalline material (associated with the coronas).

We further analyze the structural order of our system through the diffraction patterns (Fourier transform). The phases' rotational symmetry as well as the micelles' structure is revealed by these patterns as shown in the central panels of Fig. 3 for both, the cores (left) and the coronas (right). In the case of isotropic particles,  $\delta = 0$ , both patterns coincide and show the triangular symmetry of the underlying lattice as well as the peculiar staggered distribution of the particles on it. For the stripe pattern shown in Fig. 3b, where  $\delta = 0.166$ , the diffraction patterns for the cores (Fig. 3b central, left) is slightly different from the corresponding pattern for the coronas (Fig. 3b central, right) but in both cases the lane geometry is shown and not underlying triangular lattice is present, in contrast to the other cases and in accordance with the inset of Fig. 3b upper panel. As we increase the anisotropy to  $\delta = 0.333$ , the distinction between the diffraction patterns for the cores (Fig. 3c central, left) and the coronas (Fig. 3c central, right) is more clearly visible. In the first case, the internal triangular arrangement of the micelles is evident, while for the coronas this is not the case since they almost completely overlap in any given micelle. Finally, for the maximum anisotropy,  $\delta = 1$ , the disordered arrangement of the cores produces a diffuse ring in the diffraction pattern (Fig. 3d central, left) while the pattern for the coronas shows the signature of a triangular lattice (Fig. 3d central, right).

From the above results, it appears that there are two length scales associated with the pattern formation, one associated with the underlying sublattice where the cores are located (except in the case of the plastic crystal, where the core positions do not lie in a lattice) and other, associated with the coarse grained lattice or stripe patterns, where the clumps or the lanes are located. After the analysis of the radial distribution function, it is clear that this length scales are associated with the intrinsic length scales of the particles, namely, the core and corona diameters,  $\sigma_0$  and  $\lambda\sigma_0$ , respectively. However, there is a third length intrinsic to the particles which is the relative displacement between the core and the corona,  $\delta$ . Our results show that this length does not intervene in the lattice spacing but rather in the type of lattice formed: stripes, crystal, or plastic crystal. The number of particles that form the clumps or the width of a given lane are determined by the reduced density of the sample,  $\rho^*$ , and also by the shoulder width.

Two final representative patterns formed by the present model are shown in Fig. 4. Here, a zigzag pattern is shown in panel (a) for  $\lambda = 2$ ,  $\rho^* = 0.6$  and  $\delta = 0.5$ ; and a rectangular lattice of cores is shown in panel (b) for  $\lambda = 2$  and  $\delta = 0.34$ . The last example shown is obtained by means of a NPT

simulation in which the pressure is chosen so that the density is  $\rho^* = 0.7$ . Also, the shape of the simulation box is allowed to change to disregard a possible influence of the simulation box geometry on the final arrangement. Due to the simplicity of the potential it is possible to extract the lattice constants of this arrangement. The shortest axis,  $a$ , is determined by the condition  $a = \sigma_1$  while  $b = (\sqrt{3}/2) \sigma_1 + \sigma_0/2 - d$ , and this lattice can only appear if  $\lambda \geq \sqrt{3}$ . For the parameters of Fig. 4b,  $a = 2$  and  $b = 2.06$ .

### 3 Conclusions

In conclusion, we studied the self assembly of core-corona particles interacting via an anisotropic potential in two dimensions. The model contains a minimal number of geometrical parameters and despite its simplicity, it exhibits a rich variety of patterns. Among them we can highlight the formation of lanes, triangular and rectangular lattices, and unusual plastic crystals with long-range translational correlations for the coronas but with liquid-like structural features for the cores. This opens up the fascinating possibility to design an hybrid self assembled material at the nanoscale with properties that share some aspects of an amorphous and other aspects of a crystalline material. Our results indicate that the amount of anisotropy does not alter the lattice spacing and only influences the type of clustering (stripes, micells, etc.) of the individual particles. We believe that the model investigated in this work, although highly simplified contains the main ingredients to understand the self organization of discotic soft particles in 2D with anisotropic interactions.

### Acknowledgements

This work was supported in part by grant DGAPA IN-115010.

### References

- [1] Denton A., *Effective Interactions in Soft Materials*, in *Nanostructured Soft Matter: Experiment, Theory, Simulation and Perspectives*, edited by Zvelindovsky A. V. (Springer, Dordrecht, 2007), pp. 395–436.
- [2] Malescio G. Complex phase behaviour from simple potentials, *J. Phys.: Condens. Matter* **19**, 073101 (2007).
- [3] Malescio G. & Pellicane G. Stripe phases from isotropic repulsive interactions *Nature Mater.* **2**, 97-100 (2003).
- [4] Malescio G. & Pellicane G. Stripe patterns in two-dimensional systems with core-corona molecular architecture, *Phys. Rev. E* **70**, 021202 (2004).
- [5] Norizoe Y. & Kawakatsu T. Monte Carlo simulation of string-like colloidal assembly, *Europhys. Lett.* **72**, 583-589 (2005).



- [6] Camp P. J. Structure and phase behavior of a two-dimensional system with core-softened and long-range repulsive interactions, *Phys. Rev. E* **68**, 061506 (2003).
- [7] Glaser M. A., et al. Soft spheres make more mesophases, *EPL* **78**, 46004 (2007).
- [8] Fornleitner J. & Kahl G. Lane formation vs. cluster formation in two-dimensional square-shoulder systems -A genetic algorithm approach, *EPL* **82**, 18001 (2008).
- [9] Mendoza, C.I. & Batta, E. Self-assembly of binary nanoparticle dispersions: From square arrays and stripe phases to colloidal corrals, *EPL* **85**, 56004 (2009).
- [10] Lee K.J., Yoon J., & Lahann J., Recent advances with anisotropic particles, *Curr. Opin. Colloid Interface Sci.* **16**, 195 (2011).
- [11] Vanakaras, A.G. Self-organization and pattern formation of janus particles in two dimensions by computer simulations., *Langmuir* **22**, 88 (2006).
- [12] Glotzer, S.C. & Solomon, M.J. Anisotropy of building blocks and their assembly into complex structures., *Nature Mater.* **6**, 557-562 (2007).
- [13] Fejer, S.N., Chakrabarti, D., & Wales, D.J. Self-assembly of anisotropic particles, *Soft Matter* **7**, 3553 (2011).
- [14] Veerman, J.A. & Frenkel, D. Phase diagram of a system of hard spherocylinders by computer simulation, *Phys. Rev. A* **41**, 3237 (1990).
- [15] Vácha, R. & Frenkel, D. Relation between molecular shape and the morphology of self-assembling aggregates: a simulation study., *Biophys. J.* **101**, 1432 (2011).
- [16] Hong, L., Cacciuto, A., Luijten, E., & Granick, S. Clusters of Amphiphilic Colloidal Spheres, *Langmuir* **24**, 621 (2008).
- [17] Granick, S., Jiang, S., & Chen, Q. Janus particles, *Physics Today* **62**, 68 (2009).
- [18] Jiang, S., et al. Janus particle synthesis and assembly, *Adv. Mater.* **22**, 1060 (2010).
- [19] Zhang, Z. & Glotzer, S.C. Self-Assembly of Patchy Particles, *Nano Lett.* **4**, 1407 (2004).
- [20] Bianchi, E., Largo, J., Tartaglia, P., Zaccarelli, E., & Sciortino, F. Phase Diagram of Patchy Colloids: Towards Empty Liquids, *Phys. Rev. Lett.* **97**, 168301 (2006).

- [21] Bianchi, E., Blaak, R. & Likos, C. N. Patchy colloids: state of the art and perspectives, *Physical chemistry chemical physics : PCCP* **13**, 6397 (2011).
- [22] Doppelbauer, G., Bianchi, E., & Kahl, G. Self-assembly scenarios of patchy colloidal particles in two dimensions, *J. Phys.: Condens. Matter* **22**, 104105 (2010).
- [23] Pawar, A.B. & Kretzschmar, I. Fabrication, assembly, and application of patchy particles, *Macromol. Rapid Commun.* **31**, 150 (2010).
- [24] Ruzicka, B., et al. Observation of empty liquids and equilibrium gels in a colloidal clay, *Nature Mater.* **10**, 56 (2011).
- [25] Chen, Q., Bae, S.C., & Granick, S. Directed self-assembly of a colloidal kagome lattice, *Nature* **469**, 381 (2011).
- [26] Romano, F. & Sciortino, F. Two dimensional assembly of triblock Janus particles into crystal phases in the two bond per patch limit, *Soft Mat.* **7**, 5799 (2011).
- [27] Romano, F. & Sciortino, F. Colloidal self-assembly: Patchy from the bottom up, *Nature Mater.* **10**, 171 (2011).
- [28] Gay, J.G. & Berne, B.J. Modification of the overlap potential to mimic a linear site-site potential, *J. Chem. Phys.* **74**, 3316 (1981).
- [29] Frenkel, D. & Smit, B., *Understanding Molecular Simulation* (Academic, London, 1996).
- [30] Zihlerl, P. & Kamien, R.D. From lumps to lattices: crystallized clusters made simple, *J. Chem. Phys. B* **115**, 7200 (2011).

## Figure Captions

Fig. 1. Schematics of the model. Pair potential  $V(r)$  as a function of the distance  $r$  between two particles interacting via an off-centered core-corona architecture.  $r$  corresponds to the core-core distance for the hard core (blue line) and to the corona-corona distance for the square potential (red line). The upper right corner depicts the anisotropic particle. The filled blue circle represents the hard core and the red circumference is the external edge of the soft corona.

Fig. 2. Spatial arrangements of the system at temperature  $T^* = 0.01$  for  $\lambda = 2.5$  and  $\rho^* = 0.291$  (NVT simulation). (a) Stripe pattern for  $\delta = 0$ , (b) stripes mixed with a crystalline array made mainly of dimers and trimers obtained for  $\delta = 0.2$ , (c) crystalline array of dimers and trimers for  $\delta = 0.3$ , (d) plastic crystal made of a triangular array of aggregates formed mainly by two and three particles whose coronas overlap completely and can rotate independently of the other aggregates for  $\delta = 1$ .

Fig. 3. Structural properties at  $T^* = 0.01$  for  $\lambda = 3$  and  $\rho^* = 0.5$  (NVT simulation). Upper panels: Snapshots of a sequence of configurations. (a) Wiggled pattern for  $\delta = 0$ , (b) stripes for  $\delta = 0.166$ , (c) triangular lattice of heptamers for  $\delta = 0.333$ , and (d) plastic crystal made of a triangular array of aggregates formed mainly by two and three particles whose coronas overlap completely for  $\delta = 1$ . Central panels: Diffraction patterns for the cores (left) and coronas (right) for the snapshots shown in the corresponding upper panels. Bottom panels: Radial distribution function,  $g(r)$ , for the cores (blue line) and coronas (red line) for the configurations shown in the respective upper panels.

Fig. 4. Spatial arrangements of the system at temperature  $T^* = 0.01$  for  $\lambda = 2$ . (a) A zigzag pattern obtained for  $\rho^* = 0.6$  and  $\delta = 0.5$  (NVT simulation). (b) Rectangular lattice obtained for a density  $\rho^* = 0.7$  and  $\delta = 0.34$  (NPT simulation). The lines are guides for the eye to show the rectangular lattice whose parameters are  $a = 2$  and  $b = 2.06$ .

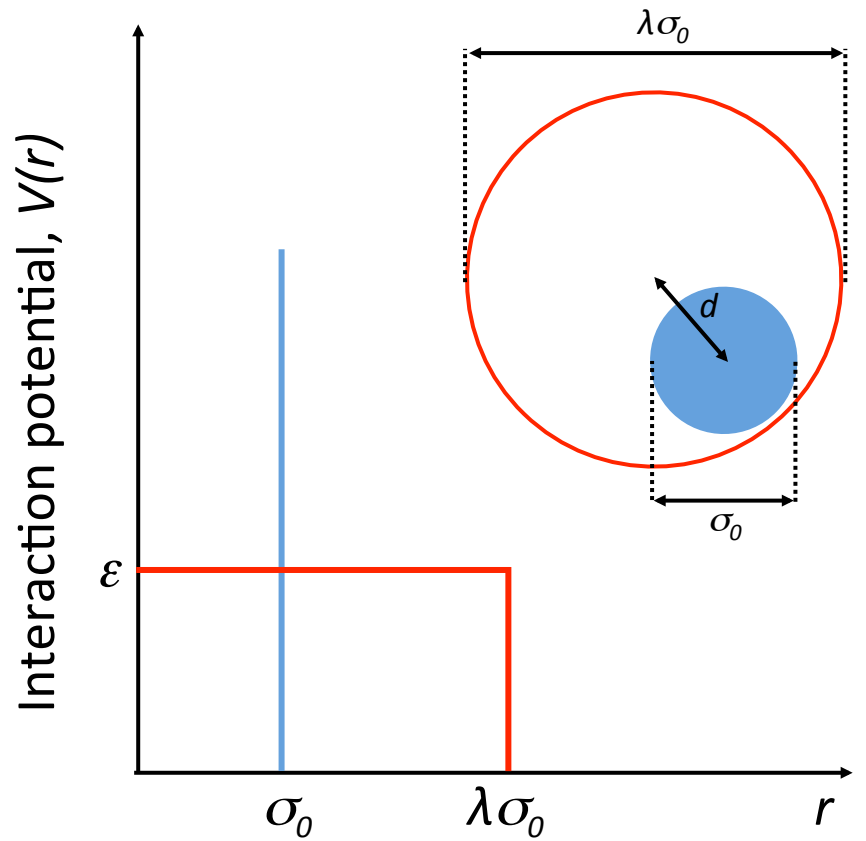


Figure 1: Schematics of the model. Pair potential  $V(r)$  as a function of the distance  $r$  between two particles interacting via an off-centered core-corona architecture.  $r$  corresponds to the core-core distance for the hard core (blue line) and to the corona-corona distance for the square potential (red line). The upper right corner depicts the anisotropic particle. The filled blue circle represents the hard core and the red circumference is the external edge of the soft corona.

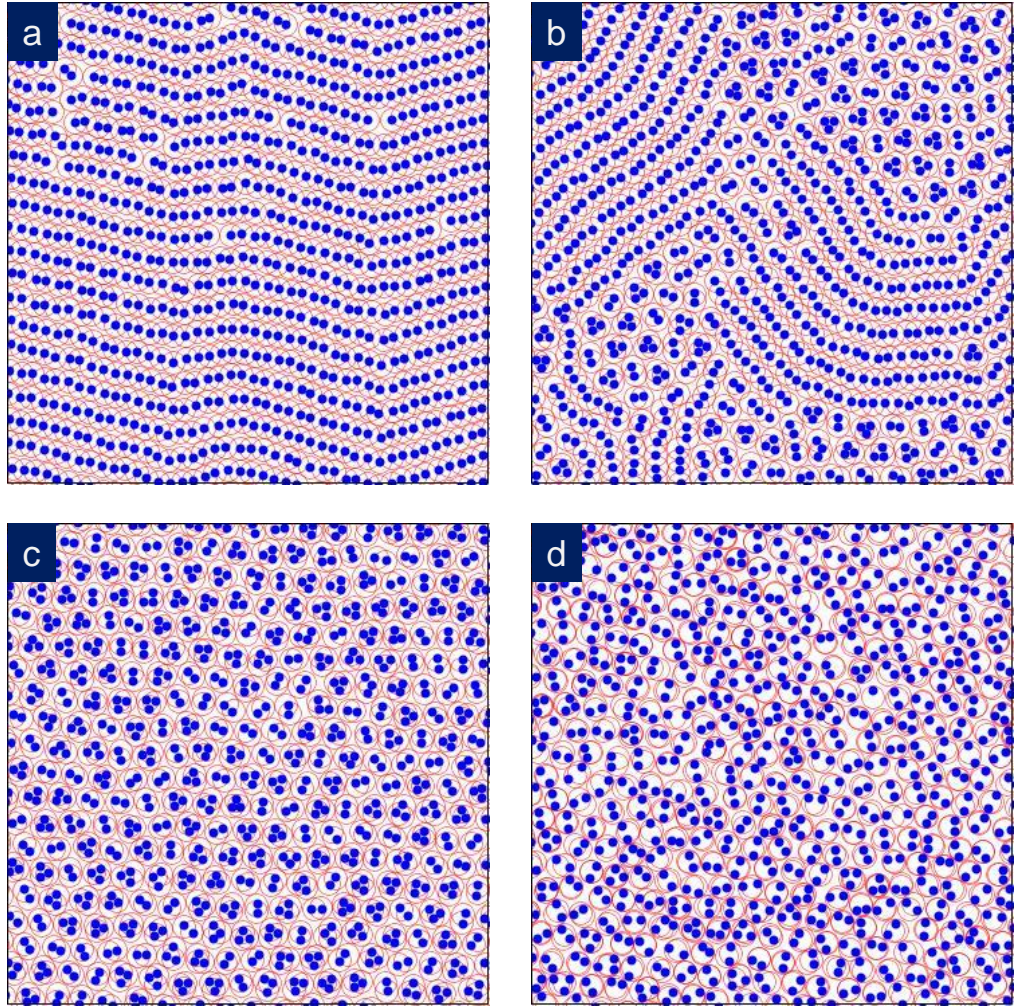


Figure 2: Spatial arrangements of the system at temperature  $T^* = 0.01$  for  $\lambda = 2.5$  and  $\rho^* = 0.291$  (NVT simulation). (a) Stripe pattern for  $\delta = 0$ , (b) stripes mixed with a crystalline array made mainly of dimers and trimers obtained for  $\delta = 0.2$ , (c) crystalline array of dimers and trimers for  $\delta = 0.3$ , (d) plastic crystal made of a triangular array of aggregates formed mainly by two and three particles whose coronas overlap completely and can rotate independently of the other aggregates for  $\delta = 1$ .

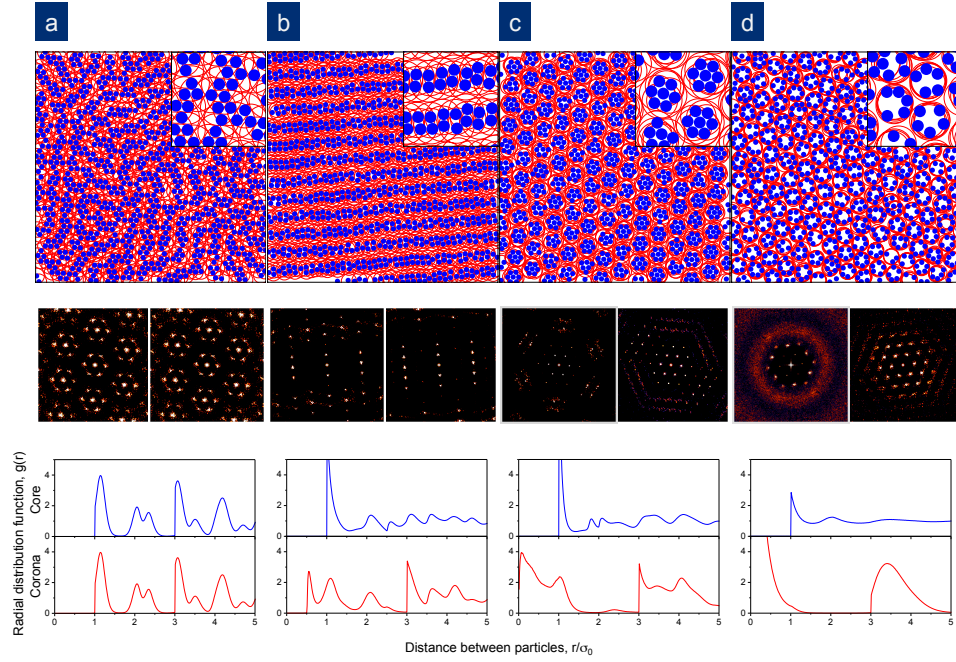


Figure 3: Structural properties at  $T^* = 0.01$  for  $\lambda = 3$  and  $\rho^* = 0.5$  (NVT simulation). Upper panels: Snapshots of a sequence of configurations. (a) Wiggled pattern for  $\delta = 0$ , (b) stripes for  $\delta = 0.166$ , (c) triangular lattice of heptamers for  $\delta = 0.333$ , and (d) plastic crystal made of a triangular array of aggregates formed mainly by two and three particles whose coronas overlap completely for  $\delta = 1$ . Central panels: Diffraction patterns for the cores (left) and coronas (right) for the snapshots shown in the corresponding upper panels. Bottom panels: Radial distribution function,  $g(r)$ , for the cores (blue line) and coronas (red line) for the configurations shown in the respective upper panels.

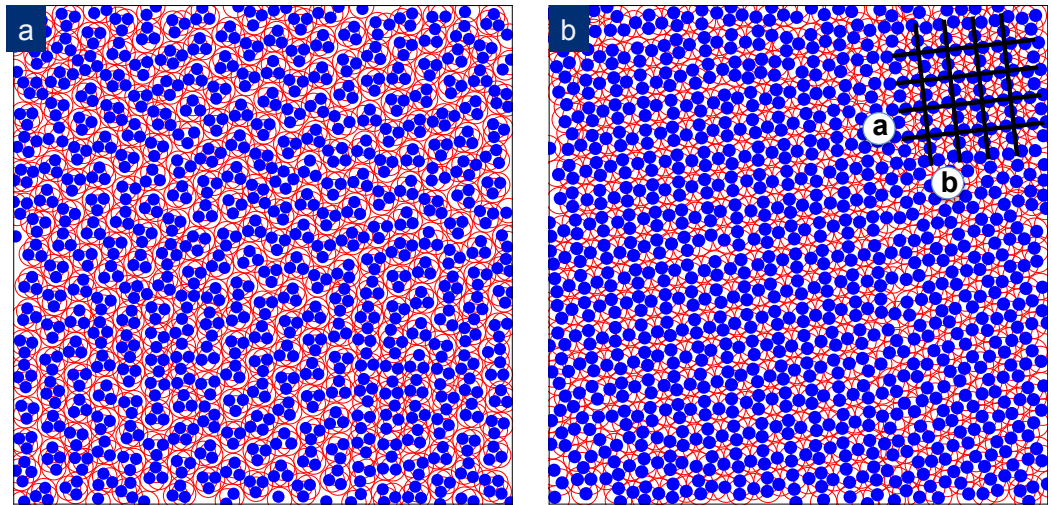


Figure 4: Spatial arrangements of the system at temperature  $T^* = 0.01$  for  $\lambda = 2$ . (a) A zigzag pattern obtained for  $\rho^* = 0.6$  and  $\delta = 0.5$  (NVT simulation). (b) Rectangular lattice obtained for a density  $\rho^* = 0.7$  and  $\delta = 0.34$  (NPT simulation). The lines are guides for the eye to show the rectangular lattice whose parameters are  $a = 2$  and  $b = 2.06$ .